



Available online freely at [www.isisn.org](http://www.isisn.org)

# Bioscience Research

Print ISSN: 1811-9506 Online ISSN: 2218-3973

Journal by Innovative Scientific Information & Services Network



RESEARCH ARTICLE

BIOSCIENCE RESEARCH, 2021 18(3): 2229-2237.

OPEN ACCESS

## Using texture analysis in brain MR imaging to differentiate between WHO Grade I and II Meningioma

Alharbi H. Turki<sup>1</sup>, Abujamea H. Abdullah<sup>\*1,2</sup> and Alsakkaf M. Hussein<sup>1</sup>

<sup>1</sup>Department of Radiology and Medical Imaging, King Saud University Medical City, Riyadh, Saudi Arabia

<sup>2</sup>Department of Radiology and Medical Imaging, College of Medicine, King Saud University, Riyadh, Saudi Arabia

\*Correspondence: [abujamea@ksu.edu.sa](mailto:abujamea@ksu.edu.sa) Received 11-06-2021, Revised: 09-08-2021, Accepted: 15-08-2021 e-Published: 16-08-2021

Differentiation between grades I and II Meningioma can be challenging in terms of radiologic features. Hence, this study uses radiomic features of 3D T1 enhanced MRI to analyze the difference between grades I and II Meningioma. A pre-operative contrast enhanced T1 images was analyzed retrospectively for 47 patients (16 grade II patients and 31 grades I). The grading of the meningioma was determined by a histo-pathologist who received samples from a neurosurgeon. Life X software which is designed to characterize tumor heterogeneity based on histogram, textural, and shape indices was used to extract the tumor features at a one and five voxel distance from neighbors. The texture indices were generated, and comparisons were made using the Weka software, which was used to calculate the sensitivity, specificity, F- score, AUROC and SPSS software was used to differentiate between WHO grades I and II of meningioma. For our dataset which consisted of 47 lesions of meningioma (31 lesions of grade I and 16 cases of grade II), For five voxel distance between neighbors, out of 17 texture features only 11 was statistically significant, namely, conventional-skewness, discretized-mean, discretized-q1, discretized-q2, discretized-q3, discretized-Skewness, GLRLM-LRHGE, GLRLM-HGRE, GLRLM-SRHGE, GLZLM-HGZE, and GLZLM-SZHGE (p-value  $\leq 0.05$ ). A random forest classifier was built after choosing the top-16 highly correlated features had a weighted sensitivity, specificity, F-score, and AUROC of 74.5%, 65.7%, 74%, and 79% respectively. For one voxel distance between neighbors, out of 17 texture features only 7 were statistically significant, namely, discretized mean, discretized\_q1, discretized\_q2, discretized\_q3, GLRLM\_LRHGE, GLRLM\_HGRE, GLRLM\_SRHGE were significant (p-value  $\leq 0.05$ ). The classifier had a weighted sensitivity, specificity, F-score, and AUROC of 78.7%, 70.4%, 78.7%, and 80%, respectively. Our results suggest that the analysis of texture and shape is potentially useful preoperative tool for WHO grades I and II differentiation of meningioma. Out of the several hundred radiomic texture characteristics extracted from the image, few features can be used for the clear discrimination between WHO grades I and II preoperatively.

**Keywords:** Magnetic Resonance Imaging, Brain, Radiomics, Meningioma, Texture Analysis.

### INTRODUCTION

Meningioma, which accounts for one-third of adult primary intracranial neoplasms, exhibits a highly varied biological behavior and is subsequently described in three grades, according to its clinical prognosis. Non-benign

meningioma, including WHO grades II and III are histologically elevated, more invasive, and proliferative (Buerki et al. 2018). Non-benign meningiomas are susceptible to progression and recurrence, despite adjuvant radiation therapy after surgical resection (Rogers et al. 2015).

Radical surgical management is preferred to achieve better results if non-benign meningiomas are diagnosed via brain MRIs (Goldbrunner et al. 2016). Thus, for planning management strategies, it is important to distinguish non-benign from benign meningioma, prospectively (Huang et al. 2019).

For noninvasive diagnosis of meningiomas, an MRI is the preferred modality. The distinction between non-benign and benign meningiomas using radiological characteristics (RCs) from conventional MRI inspection by radiologists is still difficult (Nowosielski et al. 2017). Related RCs may be predictive of non-benign meningiomas, including tumor volume, peritumoral edema, and necrosis; however, these RCs could be misinterpreted by radiologists, and the corresponding findings across studies were inconsistent (Hale et al. 2018; Lin et al. 2014). Quantitative parameters, such as diffusion tensor imaging (DTI), perfusion-weighted imaging (PWI), and diffusion-weighted imaging (DWI) were applied to the classification of meningiomas (Aslan K et al. 2018); (Surov A et al. 2015); (Toh CH et al. 2008). However, these techniques have not yet been able to identify reliable parameters for distinguishing non-benign from benign meningiomas.

Radiomics has recently been used widely for the diagnosis and prediction of clinical outcomes in brain tumors (Bi and Li, 2019); it basically involves the extraction of texture analysis (TA) from MR data. This method extracts quantitative characteristics that describe gray-level patterns, pixel interrelationships, and spectral features, most of which cannot be seen by the eye (Kassner & Thornhill, 2010). Then, these characteristics are used to construct models for machine learning to predict tumor grades and even molecular characteristics (Wang Y et al. 2019); (Zhou et al. 2018). The ability to distinguish between benign and non-benign meningiomas by using multi-parametric MRI texture models has been demonstrated in recent research studies (Lu et al. 2019); (Park JH et al. 2019); (Yan et al. 2017). However, texture models have not been validated by an independent dataset in these studies, and this may decrease the clinical benefits of these models.

Recently, some studies have presented a good impact of using texture analysis in medical imaging. Lucia's study represented the significant result of using radiomics features from DWI and positron emission tomography (PET) in advance

cervical cancer patients receiving chemo-radiotherapy (Lucia et al. 2019). Additionally, in another study of 40 confirmed glioma patients (20 low-grade glioma and 20 high-grade meningioma) with multi-parametric, the MRIs showed very significant results achieving 95% sensitivity, 95.5% accuracy, 96% specificity, and 95.5% AUROC curve (Vamvakas et al. 2019). Using multiple-parametric MRIs with TA for capturing breast intra-lesion heterogeneity offers a useful diagnostic tool for breast tumors (Tsarouchi MI et al. 2020). Furthermore, in rectal cancer study, analyzing imaging features was valuable for predicting the response of the treatment to neoadjuvant chemo-radiotherapy and tumor recurrence (Park H et al. 2020). Besides, the study of Sun which showed that the incorporation of T2w texture features significantly improved model performance for the classification of aggressiveness of prostate tumors (Sun Y et al. 2019), as well as the three types of single liver lesions (hepatic metastases (Nowosielski et al), hepatic hemangioma (Nowosielski et al.) and hepatocellular carcinoma [HCC]) could be classified using the texture features of SPAIR T2W-MRI, which can serve as an adjunct tool for accurate diagnosis of these diseases as well (Li et al. 2017). The triple-classification model of radiomics is capable of differentiating sacral giant cell tumor (SGCT), sacral chordoma (SC), and sacral metastatic tumor (SMT), which can be used in clinical practice to improve the accuracy of preoperative diagnosis (Yin et al. 2019). Moreover, the addition of traditional radiological analysis of selected radiomic attributes that quantify tumor heterogeneity and shape at baseline, in cases of myxoid/round cell liposarcomas (MRC-LPS), can improve the prediction of the prognosis of MRC-LPS patients (Crombe et al. 2020). Furthermore, with quantitative assessment of location and radiomic features on T2-weighted imaging, epilepsy presentation in unruptured brain arteriovenous malformations (bAVMs) can be predicted (Zhang et al. 2019). Also, for soft tissue sarcomas, good accuracy and AUC can be achieved using radiomic features (Corino et al. 2018).

The main purpose of the study is to test the ability of artificial intelligence to distinguish between WHO grades I and II of meningiomas and implementing it in the medical field. In this study, we also compared the ability of texture analysis in distinguishing between WHO grades I and II meningiomas from extracted texture features at one and five voxel distance from

neighbors. Format references as per journal style

## MATERIALS AND METHODS

This study was approved by Institutional Review Board (IRB) at King Saud University Medical City (IRB # 20/0720/IRB). Retrospectively, 47 patients confirmed histopathologically having meningioma were selected for this study (31 patients with grade I lesion and 16 cases with grade II lesion), table 1.

A pre-operative MRI was conducted using fluid-attenuated inversion recovery (FLAIR), DWI, T2, and 3D T1, pre- and post-Gadolinium contrast (Dotarem, Guerbet, Roissy, France). The texture analysis were applied on enhanced 3D T1 magnetization-prepared rapid gradient-echo (MPERAGE) sequence in Siemens 3T Skyra (MAGNETOM Skyra, Siemens Medical Solutions, Erlangen, Germany), (FOV = 250 mm, slice thickness = 1.04 mm, TR = 1610 ms, TE = 2.44 ms, matrix = 256 x 223). The images were extracted from PACS in a DICOM format. The images were viewed in three planes and the texture features extracted by the LifeX software (Nioche et al. 2018), which is made to analyze image heterogeneity based on the histogram, textural, and shape indices. The ROI was manually placed on tumor that was reviewed by an experienced radiologist (Figure 1). Spatial resampling spacing in x, y and z were 2 mm, 64 gray-levels in terms of intensity discretization, and ROI values were automatically rescaled between the ROI content's minimum and maximum values. To differentiate between grades I and II, we used 17 important texture features indices generated from the LifeX software (Table 2). Features including gray-level run-length matrix (GLRLM) which is the matrix from which the texture features can be pull out for texture analysis. It is a way of searching through the image across a given

direction, for group of pixels having similar gray intensity in that direction. It provides the size of homogeneous runs for each gray-level, while the grey-level zone length matrix (GLZLM) provides information on the size of homogeneous zones, and the gray-level co-occurrence matrix (GLCM) identified the image texture by calculating the number of two pixels with fixed values as well as spatial links available in an image that the GLCM can use to compute its statistical measurements (Mohanaiah et al. 2013). GLCM models the relationship among pixels inside the region by building Gray Level Co-occurrence Matrix. As per the co-occurrence matrix from our dataset, which is enhanced 3D T1 images, LIFEx extracted features in 13 directions in two types of data, depending on the voxel distance with neighbors (Haralick et al. 1973).

With the Waikato environment for knowledge analysis (Weka) software, classification analysis was conducted, using SVM learning classifiers, different classification models were constructed, and ten-fold cross-validation was used to evaluate classification performance. For each model, accuracy, sensitivity, specificity, and AUC values were calculated (Hall et al. 2009). Statistical analysis was performed using the SPSS software application with a level of significance of 0.05 (IBM Corp., 2019). In order to determine whether each texture characteristic varied significantly between WHO grade I and II meningiomas, an independent sample t-test was conducted.

In this study we analyzed one and five voxel distance between neighbors to find if there will be significant different in distinguishing grades of meningioma between one and five voxel distances. A student's t-test was used to compare statistically significant differences using one and five voxels distance from neighbors.

**Table 1: Patient Demographics**

Grade of Meningioma	Number of Patients (%)	Gender	Number of Patients (%)	Age Range
WHO Grade I	31 (65.96%)	Female	22 (70.97%)	14 - 75
		Male	9 (29.03%)	
WHO Grade II	16 (34.04%)	Female	10 (62.50%)	
		Male	6 (37.50%)	

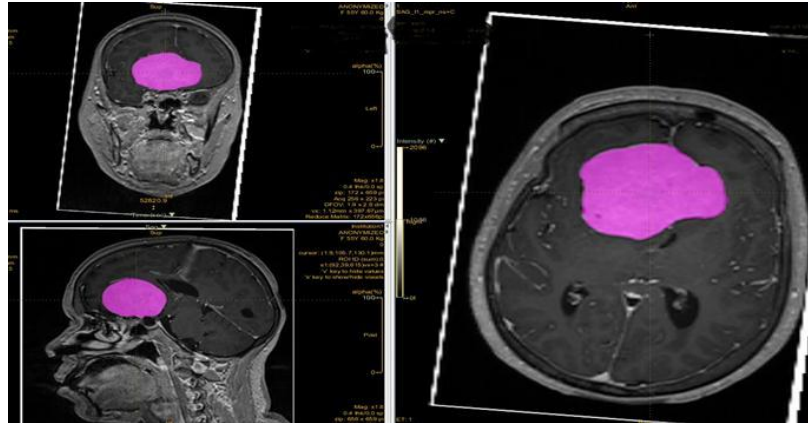


Figure 1: Screenshot of Life X software platform showing Semi-automated Meningioma segmentation.

Table 2: Texture Features extracted using LIFEx.

Feature Family	Feature Name
Grey level co-occurrence matrix (GLCM)	Homogeneity Correlation
Grey-level run length matrix (GLRLM)	Short Run Emphasis Long Run Emphasis High Grey-level Run Emphasis Short-Run High Grey-level Emphasis Long-Run High Grey-level Emphasis Run percentage
Grey-level zone length matrix (GLZLM)	High Grey-level Zone Emphasis Short-Zone High Grey-level Emphasis
Conventional/ Discretized	CONVENTIONAL skewness CONVENTIONAL min DISCRETIZED-Q1 DISCRETIZED-Q2 DISCRETIZED-Q3 DISCRETIZED skewness DISCRETIZED mean

**RESULTS**

The main aim of the study was first, to test the reliability of using TA to distinguish between grades I and II of meningioma and second, to test the ability of TA in distinguishing between WHO grades I and II meningiomas from extracted texture features using one and five voxel distance from neighbors.

**One Voxel Distance between Neighbors**

CONVENTIONAL min, CONVENTIONAL Skewness, DISCRETIZED Skewness, GLCM Homogeneity, GLCM Correlation, GLZLM\_HGZE, GLZLM\_SZHGE, GLRLM RP, GLRLM SRE, and GLRLM LRE were not significant between grades I and II (p-values were 0.746, 0.064, 0.061, 0.544, 0.23, 0.746, 0.163, 0.184, 0.628, 0.625, and 0.733, respectively), present in the independent t-test,

while DISCRETIZED mean, DISCRETIZED-Q1, DISCRETIZED-Q2, DISCRETIZED-Q3, GLRLM\_LRHGE, GLRLM\_HGRE, GLRLM\_SRHGE were significant (p-values were 0.020, 0.023, 0.008, 0.020, 0.012, 0.020, and 0.027, respectively). The classifier had a weighted sensitivity, specificity, F-score and AUROC of 78.7%, 70.4%, 78.7%, and 80%, respectively, table 3.

**Five Voxel Distance from Neighbors**

The independent t-tests for CONVENTIONAL min, GLCM Homogeneity (inverse difference), GLCM Correlation, GLRLM\_RP, GLRLM\_SRE, and GLRLM\_LRE were not significant between grades I and II (p-values were .20, .31, .79, .22, .23, and .23, respectively), while CONVENTIONAL-Skewness, DISCRETIZED-mean, DISCRETIZED-Q1, DISCRETIZED-Q2,

DISCRETIZED-Q3, DISCRETIZED Skewness, GLRLM-LRHGE, GLRLM-HGRE, GLRLM-SRHGE, GLZLM-HGZE, and GLZLM-SZHGE features were significant ( $p$ -value  $\leq 0.05$ ). Our dataset consisted of 47 lesions of meningioma (31 grade I and 16 grade II). A random forest classifier was built after choosing the top 16 highly correlated features. Using 10 cross-fold validation, the classifier showed a weighted sensitivity, specificity, F-score and AUROC of 74.5%, 65.7%, 74%, and 79%, respectively, table 4.

In table 5, A student's t-test was used to compare statistically significant differences using one and five voxels distance from neighbors to find if there is any significant different in distinguishing grades of meningioma between one and five voxel distances. It appears that CONVENTIONAL Skewness was significant at 5 voxels distance between neighbor ( $p$ -value = 0.028) but it was not significant at 1 voxel distance between neighbor ( $p$ -value= 0.064) .

**Table 3: Detailed Accuracy by Grade of Testing at 1 Voxel Distance from Neighbors**

Grade	TP rate	FP rate	Precision	Recall	F-Measure	MCC	ROC area	PRC area
I	0.848	0.357	0.848	0.848	0.848	0.491	0.80	0.897
II	0.643	0.152	0.643	0.643	0.643	0.491	0.80	0.71
Weighted avg.	0.787	0.296	0.787	0.787	0.787	0.491	0.80	0.840

\*TP: True Positive, FP: False Positive, MCC: Merchant Category Code, ROC: Receiver Operating Characteristic, PRC: Precision/Recall.

**Table 4: Detailed Accuracy by Grade of Testing at 5 Voxel Distance from Neighbor**

Grade	TP rate	FP rate	Precision	Recall	F-Measure	MCC	ROC area	PRC area
I	0.563	0.161	0.643	0.563	0.60	0.416	0.790	0.757
II	0.839	0.438	0.788	0.839	0.813	0.416	0.790	0.838
Weighted avg.	0.745	0.343	0.739	0.745	0.740	0.416	0.790	0.811

\*TP: True Positive, FP: False Positive, MCC: Merchant Category Code, ROC: Receiver Operating Characteristic, PRC: Precision/Recall.

**Table 5: Features with statistically significant differences as measured by a Student's t-test for 1 Voxel compared with 5 voxel distance from Neighbors.**

Texture Feature	1 Voxel Distance between Neighbor			5 Voxel Distance between Neighbor		
	Statistic	df*	p-value	Statistic	df*	p-value
CONVENTIONAL min	0.305	45.0	0.746	1.304	45.0	0.199
CONVENTIONAL Skewness	1.897	45.0	0.064	2.271	45.0	<b>0.028</b>
DISCRETIZED mean	-2.411	45.0	<b>0.020</b>	-2.722	45.0	<b>0.009</b>
DISCRETIZED_Q1	-2.353	45.0	<b>0.023</b>	-2.353	45.0	<b>0.023</b>
DISCRETIZED_Q2	-2.783	45.0	<b>0.008</b>	-2.475	45.0	<b>0.017</b>
DISCRETIZED_Q3	-2.413	45.0	<b>0.020</b>	-3.392	45.0	<b>0.001</b>
DISCRETIZED Skewness	1.920	45.0	0.061	2.282	45.0	<b>0.027</b>
GLCM Homogeneity [Inverse Difference]	-0.611	45.0	0.544	-1.034	35.0	0.308
GLCM Correlation	-0.326	45.0	0.746	-0.266	35.0	0.792
GLRLM_LRHGE	-2.633	45.0	0.012	-3.422	45.0	0.001
GLRLM_HGRE	-2.411	45.0	0.020	-3.273	45.0	0.002
GLRLM_SRHGE	-2.279	45.0	0.027	-3.120	45.0	0.003
GLRLM_RP	0.487	45.0	0.628	1.237	45.0	0.223
GLRLM_SRE	0.493	45.0	0.625	1.214	45.0	0.231
GLRLM_LRE	-0.344	45.0	0.733	-1.227	45.0	0.226
GLZLM_HGZE	-1.417	45.0	0.163	-2.651	45.0	<b>0.011</b>
GLZLM_SZHGE	-1.349	45.0	0.184	-2.393	45.0	<b>0.021</b>

\*df: difference variance,  $p$ -value  $\leq 0.05$  is considered significant.

DISCRETIZED Skewness was also significant at 5 voxels distance between neighbor (p-value=0.027) but it was not significant at 1 voxel distance between neighbor (p-value= 0.061). GLZLM\_HGZE and GLZLM\_SZHGE were also not significant at 1 voxel distance ( p-values= 0.163 and 0.184 respectively) but significant at 5 voxels distance (p-values of 0.011 and 0.021 respectively).

## DISCUSSION

TA is one of the main features of artificial intelligence, which when implemented in the medical field can help and accelerate patient diagnoses. In the radiology department, implementing artificial intelligence can help improve workflow, assure reliable diagnoses in some procedures, and can replace invasive ones. The primary goal of this study to implement artificial intelligence to improve the workflow and provide a reliable method of grading tumors instead of invasive procedures needing to admit the patient in the hospital.

We explored the feasibility of differentiation in this study by using texture features from MRIs, between WHO grades I and II meningiomas, using the characteristics of preoperative meningioma textures, extracted from 3D T1 enhanced images. The results of the study showed unique discrimination of features from main images between grades I and II meningiomas, with weighted sensitivity, specificity, F-score, and AUROC of 74.5%, 65.7%, 74%, and 79%, respectively. (Ke C et al. 2020) study agrees with this result, which was based on the differentiation between benign meningiomas (WHO grade I) and non-benign meningiomas (WHO grades II and III) from extracted images features of 184 patients (139 WHO grade I and 45 WHO grade II and grade III). The study showed the accuracy, sensitivity, specificity, and AUROC curve to be 80%, 84%, 78%, and 83%, respectively. These results were achieved by extracting image features from different conventional (T2w, T2-FLAIR, and T1 pre/post contrast) techniques which were not applied in our study. Moreover, Yan et al.'s research was based on texture as well as shape analysis MRI in meningiomas grading of 131 patients: 21 with high-grade meningiomas and 110 with low-grade meningiomas (Yan et al. 2017). They employed the Mann-Whitney test which showed that there were significant differences between high-grade and low-grade meningiomas in all six features. Generally, AUC values were greater than 0.50

(range, 0.73 to 0.88), while sensitivities and specificities varied from 47.62% to 90.48% and 69.09% to 96.36%, respectively. Among the nine classification models acquired, the one developed by training the SVM classifier with all six attributes accomplished the most effective performance, with a sensitivity, specificity, diagnostic accuracy and AUC of 0.86, 0.87, 0.87, and 0.87, respectively. Besides, Laukamp et al.'s study of accuracy of radiomics-based feature analysis for noninvasive meningioma grading on multiparametric MRIs of 71 meningioma patients (46 grade I and 25 grade II) concluded the study with four radiomics features that were independently identified as showing the highest predictive values for higher tumor grades: FLAIR-shape roundness (AUC = 0.80), FLAIR/T1CE-gray-level cluster shades (AUC = 0.80), DWI/ADC-gray-level variability (AUC = 0.72), and FLAIR/T1CE-gray-level-energy variability (AUC = 0.76) (Laukamp et al. 2019). The combination of the attributes resulted in an AUC of 0.91 for grade I and grade II meningiomas differentiation in a multivariate logistic regression model, which reinforces our study that it was only based on reformatted 3D T1 enhanced images. Furthermore, (Lu et al. 2019) used ADC values and texture features beside clinical and morphological features in 152 patients with meningioma, where 421 preoperative maps of ADC were included. They found that using the ADC value alone did not help distinguish the three grades of meningiomas. Equivalent diagnostic results could be achieved by machine learning classifiers based on clinical and morphological characteristics and ADC values (accuracy = 62.96%) compared to two seniors neuro-radiologists (accuracy = 61.11% and 62.04%). Moreover, Chu (2020) conducted a study predicting the WHO grade of meningiomas in 98 patients (82 cases of WHO grade I, seven cases of WHO grade II, and nine cases of WHO grade III) via extracted images features of enhanced T1WI images. The prediction results of the meningioma grade agreed with our study, with accuracy rates in the training group being 94.3%, the test group being 92.9%, the sensitivity of the training group being 94.8%, the test group being 91.7%, the specificity of training group being 91.7%, the test group being 100%, and the AUC was 0.958 and 0.948, respectively.

## CONCLUSION

Radiomic (digital image extracted texture) features provide an excellent quantitative

approach that, through appropriate spatial distribution of signal intensities and pixel interrelationships, allows excellent characterization of various regions within the same medical image. Out of the several hundred radiomic texture characteristics extracted from ROIs belonging to a group of patients. Only a few parameters selected by the operator were necessary for the clear discrimination of tumor from the surrounding tissues.

The diagnostic value of preoperative MRI was investigated in this study using texture and shape analysis for the grading of meningioma. These texture characteristics have been shown (CONVENTIONAL-Skewness, DISCRETIZED-mean, DISCRETIZED-Q1, DISCRETIZED-Q2, DISCRETIZED-Q3, DISCRETIZED-Skewness, GLRLM-LRHGE, GLRLM-HGRE, GLRLM-SRHGE, GLZLM-HGZE, and GLZLM-SZHGE) to be of help in determining the grade of meningioma. Classifying models built with these characteristics generally yielded satisfactory results. The results of this study suggest that analysis of texture and shape are potentially useful tools for clinical practice preoperative differentiation of WHO grades I and II meningiomas.

#### CONFLICT OF INTEREST

The authors declared that present study was performed in absence of any conflict of interest.

#### ACKNOWLEDGEMENT

We would like to express a great appreciation to Dr Metab Alkubeyyer for his valuable and constructive suggestions during the planning and development of this research work. His willingness to give his time so generously has been very much appreciated.

#### AUTHOR CONTRIBUTIONS

Both first and second authors contributed equally to this work.

#### Copyrights: © 2021@ author (s).

This is an open access article distributed under the terms of the [Creative Commons Attribution License \(CC BY 4.0\)](https://creativecommons.org/licenses/by/4.0/), which permits unrestricted use, distribution, and reproduction in any medium, provided the original author(s) and source are credited and that the original publication in this journal is cited, in accordance with accepted academic practice. No use, distribution or reproduction is permitted which does not comply

with these terms.

#### REFERENCES

- Aslan K, Gunbey HP, Tomak L & Incesu L. (2018). The diagnostic value of using combined MR diffusion tensor imaging parameters to differentiate between low- and high-grade meningioma. *Br J Radiol*, 91(1088), 20180088. <https://doi.org/10.1259/bjr.20180088>
- Bi Y & Li L. (2019). Pathologically confirmed brain metastases from primary uterine cervical tumors: two cases and a literature review. *World J Surg Oncol*, 17(1), 174. <https://doi.org/10.1186/s12957-019-1720-7>
- Buerki RA, Horbinski CM, Kruser T, Horowitz PM, James CD & Lukas RV. (2018). An overview of meningiomas. *Future Oncol*, 14(21), 2161-2177. <https://doi.org/10.2217/fon-2018-0006>
- Corino VDA, Montin E, Messina A, Casali PG, Gronchi A, Marchiano A & Mainardi LT. (2018). Radiomic analysis of soft tissues sarcomas can distinguish intermediate from high-grade lesions. *J Magn Reson Imaging*, 47(3), 829-840. <https://doi.org/10.1002/jmri.25791>
- Crombe A, Le Loarer F, Sitbon M, Italiano A, Stoeckle E, Buy X & Kind M. (2020). Can radiomics improve the prediction of metastatic relapse of myxoid/round cell liposarcomas? *Eur Radiol*, 30(5), 2413-2424. <https://doi.org/10.1007/s00330-019-06562-5>
- Goldbrunner R, Minniti G, Preusser M, Jenkinson MD, Sallabanda K, Houdart E, von Deimling A, Stavrinou P, Lefranc F, Lund-Johansen M, Moyal EC, Brandsma D, Henriksson R, Soffietti R & Weller M. (2016). EANO guidelines for the diagnosis and treatment of meningiomas. *Lancet Oncol*, 17(9), e383-391. [https://doi.org/10.1016/S1470-2045\(16\)30321-7](https://doi.org/10.1016/S1470-2045(16)30321-7)
- Hale AT, Wang L, Strother MK & Chambless LB. (2018). Differentiating meningioma grade by imaging features on magnetic resonance imaging. *J Clin Neurosci*, 48, 71-75. <https://doi.org/10.1016/j.jocn.2017.11.013>
- Hall M, Frank E, Holmes G, Pfahringer B, Reutemann P & Witten I. (2009). The WEKA data mining software: an update. *ACM SIGKDD Explorations Newsletter*, 11(1).
- Haralick R, Haralick K & Dinstein I. (1973). Textural features for image classification. *IEEE Transactions on Systems, Man, and Cybernetics SMC-3*, 6, 610-621.

- Huang RY, Unadkat P, Bi WL, George E, Preusser M, McCracken JD, Keen JR, Read WL, Olson JJ, Seystahl K, Le Rhun E, Roelcke U, Koeppen S, Furtner J, Weller M, Raizer JJ, Schiff D & Wen PY. (2019). Response assessment of meningioma: 1D, 2D, and volumetric criteria for treatment response and tumor progression. *Neuro Oncol*, 21(2), 234-241. <https://doi.org/10.1093/neuonc/noy126>
- Kassner A & Thornhill RE. (2010). Texture analysis: a review of neurologic MR imaging applications. *AJNR Am J Neuroradiol*, 31(5), 809-816. <https://doi.org/10.3174/ajnr.A2061>
- Ke C, Chen H, Lv X, Li H, Zhang Y, Chen M, Hu D, Ruan G, Zhang Y, Zhang Y, Liu L & Feng Y. (2020). Differentiation Between Benign and Nonbenign Meningiomas by Using Texture Analysis From Multiparametric MRI. *J Magn Reson Imaging*, 51(6), 1810-1820. <https://doi.org/10.1002/jmri.26976>
- Laukamp KR, Shakirin G, Baessler B, Thiele F, Zopfs D, Grosse Hokamp N, Timmer M, Kabbasch C, Perkuhn M & Borggreffe J. (2019). Accuracy of Radiomics-Based Feature Analysis on Multiparametric Magnetic Resonance Images for Noninvasive Meningioma Grading. *World Neurosurg*, 132, e366-e390. <https://doi.org/10.1016/j.wneu.2019.08.148>
- Li Z, Mao Y, Huang W, Li H, Zhu J, Li W & Li B. (2017). Texture-based classification of different single liver lesion based on SPAIR T2W MRI images. *BMC Med Imaging*, 17(1), 42. <https://doi.org/10.1186/s12880-017-0212-x>
- Lin BJ, Chou KN, Kao HW, Lin C, Tsai WC, Feng SW, Lee MS & Hueng DY. (2014). Correlation between magnetic resonance imaging grading and pathological grading in meningioma. *J Neurosurg*, 121(5), 1201-1208. <https://doi.org/10.3171/2014.7.JNS132359>
- Lu Y, Liu L, Luan S, Xiong J, Geng D & Yin B. (2019). The diagnostic value of texture analysis in predicting WHO grades of meningiomas based on ADC maps: an attempt using decision tree and decision forest. *Eur Radiol*, 29(3), 1318-1328. <https://doi.org/10.1007/s00330-018-5632-7>
- Lucia F, Visvikis D, Vallieres M, Desseroit MC, Miranda O, Robin P, Bonaffini PA, Alfieri J, Masson I, Mervoyer A, Reinhold C, Pradier O, Hatt M & Schick U. (2019). External validation of a combined PET and MRI radiomics model for prediction of recurrence in cervical cancer patients treated with chemoradiotherapy. *Eur J Nucl Med Mol Imaging*, 46(4), 864-877. <https://doi.org/10.1007/s00259-018-4231-9>
- Mohanaiah P, Sathyanarayana P & GuruKumar L. (2013). Image Texture Feature Extraction Using GLCM Approach. *International Journal of Scientific and Research Publications*, 3(5).
- Nioche C, Orhac F, Boughdad S, Reuze S, Goya-Outi J, Robert C, Pellot-Barakat C, Soussan M, Frouin F & Buvat I. (2018). LIFEx: A Freeware for Radiomic Feature Calculation in Multimodality Imaging to Accelerate Advances in the Characterization of Tumor Heterogeneity. *Cancer Res*, 78(16), 4786-4789. <https://doi.org/10.1158/0008-5472.CAN-18-0125>
- Nowosielski M, Galdiks N, Iglseider S, Kickingereder P, von Deimling A, Bendszus M, Wick W & Sahm F. (2017). Diagnostic challenges in meningioma. *Neuro Oncol*, 19(12), 1588-1598. <https://doi.org/10.1093/neuonc/nox101>
- Park H, Kim KA, Jung JH, Rhie J & Choi SY. (2020). MRI features and texture analysis for the early prediction of therapeutic response to neoadjuvant chemoradiotherapy and tumor recurrence of locally advanced rectal cancer. *Eur Radiol*, 30(8), 4201-4211. <https://doi.org/10.1007/s00330-020-06835-4>
- Park JH, Bae YJ, Choi BS, Jung YH, Jeong WJ, Kim H, Sunwoo L, Jung C & Kim JH. (2019). Texture Analysis of Multi-Shot Echo-planar Diffusion-Weighted Imaging in Head and Neck Squamous Cell Carcinoma: The Diagnostic Value for Nodal Metastasis. *J Clin Med*, 8(11). <https://doi.org/10.3390/jcm8111767>
- Proctor DT, Ramachandran S, Lama S & Sutherland GR. (2018). Towards Molecular Classification of Meningioma: Evolving Treatment and Diagnostic Paradigms. *World Neurosurg*, 119, 366-373. <https://doi.org/10.1016/j.wneu.2018.08.019>
- Rogers L, Barani I, Chamberlain M, Kaley TJ, McDermott M, Raizer J, Schiff D, Weber DC, Wen PY & Vogelbaum MA. (2015). Meningiomas: knowledge base, treatment outcomes, and uncertainties. A RANO review. *J Neurosurg*, 122(1), 4-23. <https://doi.org/10.3171/2014.7.JNS131644>
- Sun Y, Reynolds HM, Wraith D, Williams S, Finnegan ME, Mitchell C, Murphy D & Haworth A. (2019). Automatic stratification of

- prostate tumour aggressiveness using multiparametric MRI: a horizontal comparison of texture features. *Acta Oncol*, 58(8), 1118-1126. <https://doi.org/10.1080/0284186X.2019.1598576>
- Surov A, Gottschling S, Mawrin C, Prell J, Spielmann RP, Wienke A & Fiedler E. (2015). Diffusion-Weighted Imaging in Meningioma: Prediction of Tumor Grade and Association with Histopathological Parameters. *Transl Oncol*, 8(6), 517-523. <https://doi.org/10.1016/j.tranon.2015.11.012>
- Toh CH, Castillo M, Wong AM, Wei KC, Wong HF, Ng SH & Wan YL. (2008). Differentiation between classic and atypical meningiomas with use of diffusion tensor imaging. *AJNR Am J Neuroradiol*, 29(9), 1630-1635. <https://doi.org/10.3174/ajnr.A1170>
- Tsarouchi MI, Vlachopoulos GF, Karahaliou AN, Vassiou KG & Costaridou LI. (2020). Multiparametric MRI lesion heterogeneity biomarkers for breast cancer diagnosis. *Phys Med*, 80, 101-110. <https://doi.org/10.1016/j.ejmp.2020.10.007>
- Vamvakas A, Williams SC, Theodorou K, Kapsalaki E, Fountas K, Kappas C, Vassiou K & Tsougos I. (2019). Imaging biomarker analysis of advanced multiparametric MRI for glioma grading. *Phys Med*, 60, 188-198. <https://doi.org/10.1016/j.ejmp.2019.03.014>
- Wang Y, Hu D, Yu H, Shen Y, Tang H, Kamel IR & Li Z. (2019). Comparison of the Diagnostic Value of Monoexponential, Biexponential, and Stretched Exponential Diffusion-weighted MRI in Differentiating Tumor Stage and Histological Grade of Bladder Cancer. *Acad Radiol*, 26(2), 239-246. <https://doi.org/10.1016/j.acra.2018.04.016>
- Yan PF, Yan L, Hu TT, Xiao DD, Zhang Z, Zhao HY & Feng J. (2017). The Potential Value of Preoperative MRI Texture and Shape Analysis in Grading Meningiomas: A Preliminary Investigation. *Transl Oncol*, 10(4), 570-577. <https://doi.org/10.1016/j.tranon.2017.04.006>
- Yin P, Mao N, Zhao C, Wu J, Chen L & Hong N. (2019). A Triple-Classification Radiomics Model for the Differentiation of Primary Chordoma, Giant Cell Tumor, and Metastatic Tumor of Sacrum Based on T2-Weighted and Contrast-Enhanced T1-Weighted MRI. *J Magn Reson Imaging*, 49(3), 752-759. <https://doi.org/10.1002/jmri.26238>
- Zhang Y, Yan P, Liang F, Ma C, Liang S & Jiang C. (2019). Predictors of Epilepsy Presentation in Unruptured Brain Arteriovenous Malformations: A Quantitative Evaluation of Location and Radiomics Features on T2-Weighted Imaging. *World Neurosurg*, 125, e1008-e1015. <https://doi.org/10.1016/j.wneu.2019.01.229>
- Zhou M, Scott J, Chaudhury B, Hall L, Goldgof D, Yeom KW, Iv M, Ou Y, Kalpathy-Cramer J, Napel S, Gillies R, Gevaert O & Gatenby R. (2018). Radiomics in Brain Tumor: Image Assessment, Quantitative Feature Descriptors, and Machine-Learning Approaches. *AJNR Am J Neuroradiol*, 39(2), 208-216. <https://doi.org/10.3174/ajnr.A5391>